Chinese Chemical Letters 35 (2024) 108638

Contents lists available at ScienceDirect

Chinese Chemical Letters

journal homepage: www.elsevier.com/locate/cclet

Boosting the performance of $LiNi_{0.90}Co_{0.06}Mn_{0.04}O_2$ electrode by uniform Li_3PO_4 coating *via* atomic layer deposition

Mingjiao Lu[a], Zhixing Wang[a,c,d], Gui Luo[b], Huajun Guo[a,c,d], Xinhai Li[a,c,d], Guochun Yan[a,d], Qihou Li[a], Xianglin Li[e], Ding Wang[f], Jiexi Wang[a,c,d,*]

[a] School of Metallurgy and Environment, Central South University, Changsha 410083, China
[b] BASF ShanShan Battery Materials Co., Ltd., Changsha 410006, China
[c] Engineering Research Center of the Ministry of Education for Advanced Battery Materials, Central South University, Changsha 410083, China
[d] Hunan Provincial Key Laboratory of Nonferrous Value-Added Metallurgy, Central South University, Changsha 410083, China
[e] School of Physics and Chemistry, Hunan First Normal University, Changsha 410205, China
[f] National and Local Joint Engineering Laboratory for Lithium-ion Batteries and Materials Preparation Technology, Key Laboratory of Advanced Battery Materials of Yunnan Province, Faculty of Metallurgical and Energy Engineering, Kunming University of Science and Technology, Kunming 650093, China

ARTICLE INFO

Article history:
Received 24 April 2023
Revised 18 May 2023
Accepted 31 May 2023
Available online 2 June 2023

Keywords:
Ultra-high nickel material
$LiNi_{0.90}Co_{0.06}Mn_{0.04}O_2$
Atomic layer deposition
Li_3PO_4
Ionic conductor

ABSTRACT

Ultra-high nickel material is considered to be a promising cathode material. However, with the increase of nickel content, the interfacial side reactions between the cathode and electrolyte become increasingly serious. Herein, an atomically controllable ionic conductor Li_3PO_4 (LPO) coating is deposited on the $LiNi_{0.90}Co_{0.06}Mn_{0.04}O_2$ (NCM9064) based electrode by the atomic layer deposition method. The results shows that the LPO coating is uniformly and densely covered on the surface of secondary particles of NCM9064, helping to prevent the direct contact between the electrolyte and cathode during the charging-discharging process. In addition, the coating layer is electrochemically stable. As a result, the interfacial side reactions during the long cycle are effectively suppressed, and the solid electrolyte interphase layer at the interface is stabilized. The electrode with 20 layers of LPO deposition (ALD-LPO-20) exhibits an excellent capacity retention of 81% after 200 cycles in 2.8-4.3 V at 25 °C, which is 18% higher than the unmodified material (ALD-LPO-0). Besides, the moderate LPO coating improves the rate capability and high temperature cycling performance of NCM9064. This study provides a method for the modification of ultra-high nickel cathode materials and corresponding electrodes.

The development of electric vehicle has been largely promoted by lithium-ion batteries (LIBs) [1]. Cathode materials have attracted extensive attention as a key part of LIBs. Among the numerous cathode materials, nickel-rich layered cathode material has been widely studied because it possesses high energy density, high working potential and low price [2–4]. However, with the increasing of nickel content, nickel-rich cathode materials exhibit more terrible cycling stability and worse rate capability [5,6]. Generally, the poor electrochemical performance for nickel-rich cathode materials can be summarized as the following reasons: (1) Phase transition occurring inside the material during charging and discharging, and (2) interfacial side reactions between the cathode material and the electrolyte [7].

In order to address above mentioned issues, strategies including surface modification [8–10], element doping [11–13] and new electrolytes [14–16] have been widely investigated. Generally speaking, as for Ni-rich cathode materials, surface modification has a greater impact on the cathode materials than internal structure stabilization [17]. Coating can prevent the electrolyte from directly contacting with cathode materials, suppressing the electrolyte decomposition and interface deterioration [18,19]. However, it is difficult to obtain a uniform but controllable coating layer on whole particle surface simultaneously by traditional wet or dry coating process [20]. Recently, the atomic layer deposition (ALD) has been used in surface coating of layered cathode materials including $LiNi_{1/3}Co_{1/3}Mn_{1/3}O_2$ [21], $LiNi_{0.5}Co_{0.2}Mn_{0.3}O_2$ [22], $LiNi_{0.6}Co_{0.2}Mn_{0.2}O_2$ [23], $LiNi_{0.8}Co_{0.1}Mn_{0.1}O_2$ [24,25] and $LiNi_{0.8}Co_{0.1}Al_{0.05}O_2$ [26]. The types of coatings include oxides [27,28], ionic conductors [29], fluorides [30], *etc.*

However, the above-mentioned coating on powder material, and often results in the lower speed of electron transport among particles [19]. On the contrary, the electron transport path of particle is not destroyed if the coating is immediately applied to

* Corresponding author.
E-mail address: wangjiexikeen@csu.edu.cn (J. Wang).

https://doi.org/10.1016/j.cclet.2023.108638
1001-8417/

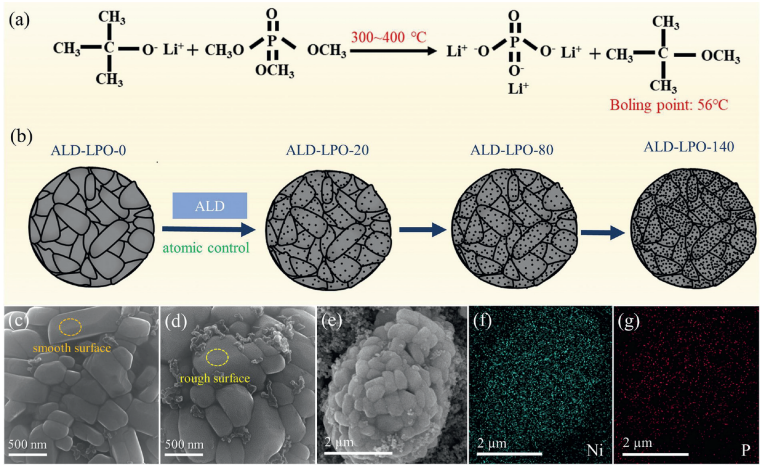

Fig. 1. (a) Reaction mechanism for ALD of LPO. (b) Schematic illustration for the progress of ALD of LPO on the surface of NCM9064 electrode. Magnified SEM images showing the surface change of samples (c) before and (d) after LPO coating. (e-g) EDS mappings of LPO-coated NCM9064 electrode.

the electrode. In the current study, methods for electrode coating mainly includes magnetron sputtering (MS) and ALD. Electrode coating by ALD is similar to particle coating. Ahn *et al.* [31] and Liu *et al.* [32] separately prepared an ultra-thin ZrO_2 coating on the surface of $LiNi_{0.5}Co_{0.2}Mn_{0.3}O_2$ and $LiNi_{0.6}Co_{0.2}Mn_{0.2}O_2$ electrodes by ALD, producing a stable surface and improving the cycle and rate properties. Liang *et al.* [33] coated the surface of the $LiNi_{0.8}Co_{0.1}Mn_{0.1}O_2$ (NCM811) electrode with a high-voltage-stabilized solid electrolyte layer lithium niobium oxide (LNO) by ALD to stabilize the cathode-PEO solid polymer interface. With LNO coating, the chemical mechanical degradation and oxygen release can be inhibited, and the decomposition of PEO can be mitigated. Although the oxide coating materials can alleviate some side reactions, they always limit the migration of lithium ions and lead to the increase of polarization. To overcome this problem, some fast ionic conductors have been studied due to their good ionic conductivity, such as the $LiNbO_3$ coating mentioned above [33]. In addition, Deng *et al.* [34] reported the Li_3PO_4 coating deposited on the surface of NCM811 powders by atomic layer deposition, to solve the problem of incompatible interface between cathode materials and sulfide-based solid electrolytes. Although ALD has been studied on nickel-rich material as well as cathodes, Li_3PO_4(LPO) deposition on $LiNi_{0.90}Co_{0.06}Mn_{0.04}O_2$ (NCM9064) electrode has not been reported. Compared with NCM811, NCM9064 can provide higher capacity and meet the requirements of high energy density. Therefore, the study of NCM9064 electrode is of great significance for realizing longer endurance of electric vehicles.

In this work, for achieving a uniform and controllable coating layer on the NCM9064 cathode, the ionic conductor LPO coating is fabricated on NCM9064 cathode by ALD. Through repeating the coating cycle, the coating thickness can be regulated accurately. As a chemical inert layer, the introduced LPO with strong P-O chemical bond is electrochemically stable at high voltage, and will not react with the HF decomposed by the electrolyte. As such, it acts as a physical barrier to prevent direct contact between the cathode and electrolyte, beneficial to suppressing the side reaction at the interface. It is expected that the cycling and rate performance of NCM9064 cathode can be improved and the microcracks in the cathode particles can be reduced.

As demonstrated in Fig. 1a, the ALD reaction is designed between LiOtBu and TMPO at 300 °C, in which process LPO are homogenously deposited while the by-product C(CH3)3OCH3 evaporates above 56 °C. In gas phase reaction, the product LPO are able to homogeneously precipitate on the surface of NCM9064 electrode by controlling the depositing layer (Fig. 1b). The crystal structure would not change during ALD process (Fig. S1 and Table S1 in Supporting information). The shape of NCM9064 secondary spheres of before and after modification does not change (Fig. S2 in Supporting information), which are primary particles with different sizes. However, under a larger magnification (Figs. 1c and d), difference can be found on the surface of primary particles. Particularly, the primary particles are smooth before ALD coating while rough surface closely attached with nanoparticles can be seen after modification. The ultra-small particle layer is proposed to be deposited LPO, which is verified by the EDS mapping of P (Figs. 1e-g and Fig. S3 in Supporting information) and XPS curve of P 2p (Fig. S4 in Supporting information).

To evaluate the effect of LPO coating on the electrochemical performance of NCM9064 cathode, charge and discharge measurements were enforced in half-cells under 25 and 45 °C. As shown in Fig. 2a and Table S2 (Supporting information), the initial discharge capacities at 0.1 C (1 C = 200 mAh/g) are 220.2, 213.9, 208.4 and 202.3 mAh/g with the initial coulombic efficiencies (ICEs) of 78.9%, 87.0%, 84.1% and 83.7% for ALD-LPO-0, ALD-LPO-20, ALD-LPO-80 and ALD-LPO-140, respectively. After LPO coating, the electrode shows much improved ICE. In addition, too many LPO layer would lead to a slight decline in initial discharge capacities due to electrochemically inert property of LPO. Fig. 2b shows the cycle performance of as-prepared sample at 25 °C. The initial capacities of ALD-LPO-0, ALD-LPO-20, ALD-LPO-80 and ALD-LPO-140 at 1 C are 202.1, 201.6, 192.8 and 184.2 mAh/g, respectively. Their discharge specific capacities after 200 cycles are separately 127.9, 161.4, 158.5 and 145.3 mAh/g, corresponding to the capacity retentions of 63%, 81%, 82% and 79%. Particularly, compared with the uncoated material, the discharge specific capacity of the ALD-LPO-20 material after 200 cycles is increased by 33 mAh/g, and the cycle retention is improved by 18%. It is noted that when the ALD-LPO-140 shows much enlarged polarization, which may be because of the residual organic by-products on the surface of electrode. When performed at elevated temperature (45 °C), the samples all show much improved reversible capacities at both 0.1 and 1 C rates (Figs. 2c and d, Table S3 in Supporting information) while decay faster as compared to those at room temperature (25 °C). Particularly, ALD-LPO-0, ALD-LPO-20, ALD-LPO-80 and ALD-LPO-140 exhibit 212.8, 218.5, 218.5 and 209.2 mAh/g at 1 C rate and maintain capacity retention of 67%, 72%, 79% and 70%, respectively after 100 cycles. Note that, with the increase of deposition layers, the capacity retention shows a trend of firstly increasing and then decreasing. Therefore, the coating layer can neither be too thin nor too thick. Coating layers is too thin to protect the material well. If the number of

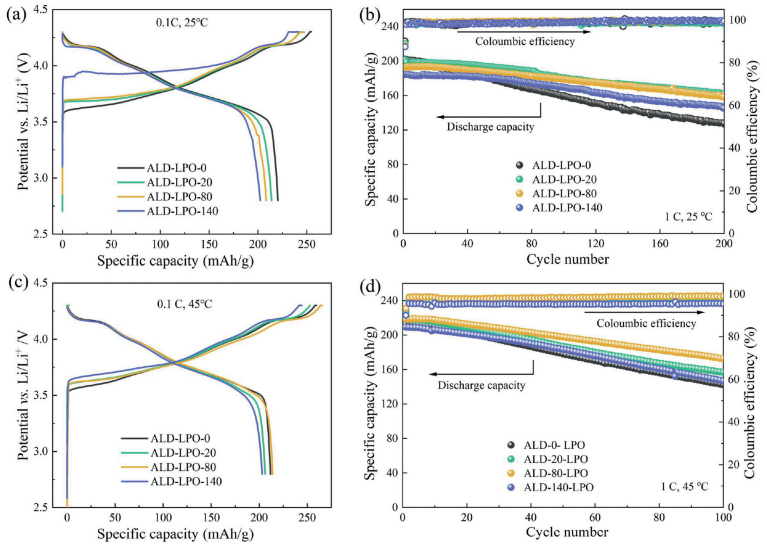

Fig. 2. (a, c) Initial charge-discharge curves at 0.1 C and (b, d) cycle performance at 1 C of as-prepared samples under different temperatures: (a, b) 25 °C and (c, d) 45 °C.

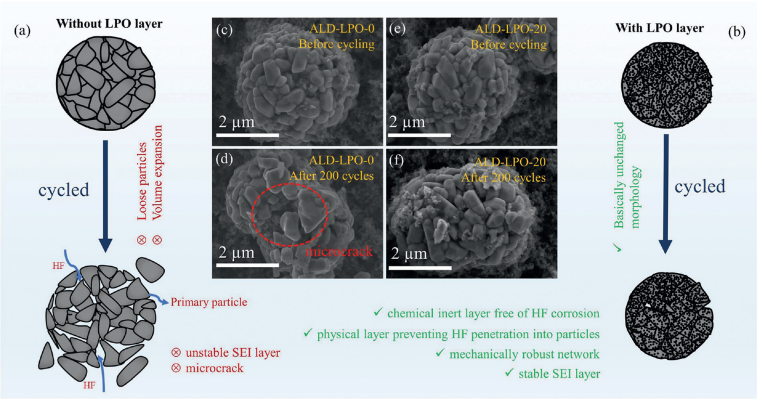

Fig. 3. Schematic diagram for explaining the roles of LPO coating layer on improving the cycling performance of NCM9064 cathode: (a) without LPO layer, (b) with LPO layer; SEM images of (c, d) ALD-LPO-0 and (e, f) ALD-LPO-20 electrodes (c, e) before cycling and (d, f) after 200 cycles.

coating layers is too thick, the specific discharge capacity will be sacrificed. Therefore, it is necessary to find a balance between the discharge capacity and the capacity retention, and to optimize the number of coating layers. It can be concluded that the ALD-LPO-80 shows the best comprehensive cycling performance. When cycling at high temperature, more intense side reactions occur at the interface between the cathodes and the electrolyte [35]. Moreover, Ni^{4+} at high de-lithiation state results in oxygen release, causing poor thermal stability of the material [36]. Therefore, compared with room temperature, thicker coating layer is needed to slow down the side reactions at the interface. Rate performance of samples (Fig. S5 in Supporting information) indicates that all samples show decay trend as the current density increases. However, the attenuation trend of ALD-LPO-80 and ALD-LPO-140 is larger while that of ALD-LPO-20 is smaller compared with that of ALD-LPO-0. Particularly, ALD-LPO-20 can still deliver a higher capacity of 174.6 mAh/g at 5 C, which is 7.0 mAh/g larger than that of ALD-LPO-0. This is because the appropriate coating layer not only does not hinder the migration of lithium ions in the charging and discharging process under high current density, but also well protect the cathode/electrolyte interface and reduce the occurrence of side reactions.

It can be concluded that no matter at 25 °C or 45 °C, the LPO coated electrodes show improved cycle stability than the bare one. It is because that LPO layer plays crucial roles at the interface of cathode and electrolyte. As compared in Figs. 3a and b, on one hand, the LPO acts as a physical barrier layer to build a mechanically robust network (as mentioned in Fig. 1), helping to reduce the stress expansion of whole cathode and prevent HF penetration into particles. On the other hand, it performs as a chemical inert and electrochemically stable layer with strong P-O chemical bond and fast lithium ion conducting property, benefiting to constructing a stable solid electrolyte interphase (SEI) film free of HF corrosion. To verify the above hypothesis, the morphologies of the samples before cycling and after 200 cycles are presented in Figs. 3c-f. It can be seen that the particles in ALD-LPO-0 have obvious cracks while ALD-LPO-20 presents fine particles with almost no obvious microcracks. The results reveal that microcracks of the secondary particles are relieved after coating from the microscopic point of view.

$$LiPF_6 \rightarrow LiF + PF_5 \quad (1)$$

$$PF_5 + H_2O \rightarrow POF_3 + 2HF \quad (2)$$

$$2POF_3 + 3Li_2O \rightarrow 6LiF + P_2O_5 \text{ (or } Li_xPOF_y) \quad (3)$$

In order to study the special chemical composition of SEI film on the surface of electrodes, taking ALD-LPO-0 and ALD-LPO-20 as

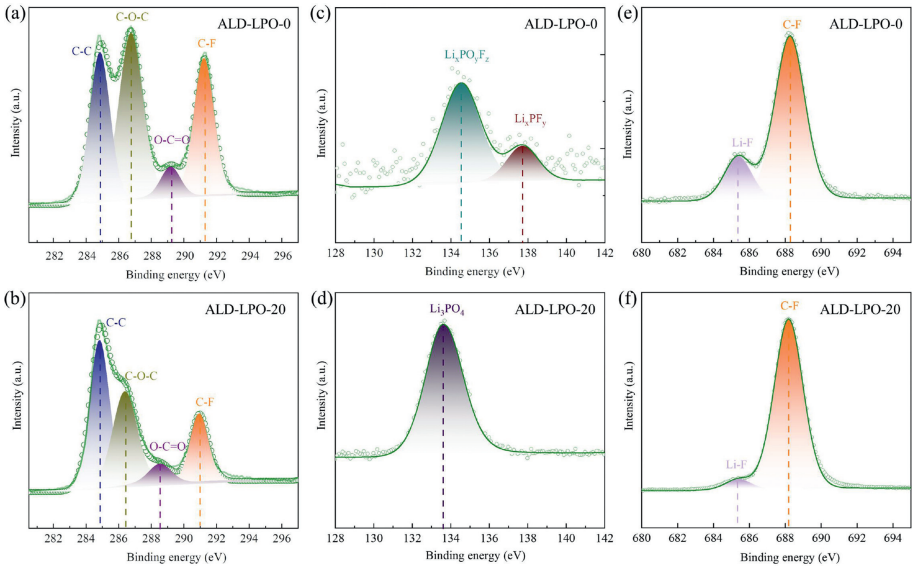

Fig. 4. High-resolution XPS spectra of (a, b) C 1s, (c, d) P 2p, and (e, f) F 1s of (a, c, e) the ALD-LPO-0 and (b, d, f) ALD-LPO-20 electrodes.

examples for comparison, the cycled NCM9064 electrodes without and with LPO layer were characterized by XPS (Figs. 4a-f). In C 1s XPS (Figs. 4a and b), the peak of C-C (284.85 eV) is attributed to C-C from the super pll [37,38]. The peaks at 286.50-286.80 eV (C-O-C) and 288.56-289.21 eV (O-C=O) are appointed primarily to the decomposition of carbonate solvent, the byproducts of organic solvent decomposition include organic alkyl lithium carbonate ($ROCO_2Li$) and lithium carbonate (Li_2CO_3) [39], while C-F peaks at 290.96-291.25 eV makes up PVDF binder [40]. In Fig. 4c, the P 2p XPS curve of ALD-LPO-0 shows that the detected chemical bonds O-P-F ($Li_xPO_yF_z$) [41] and P-F(Li_xPF_y) [42] separately at 134.52 eV and 137.73 eV are derived from the decomposition of $LiPF_6$. However, these chemical bonds are not detected at the cathode surface of ALD-LPO-20, and only the P-O of Li_3PO_4 is collected (Fig. 4d). It is because that the P-O bond has a stronger peak than O-P-F ($Li_xPO_yF_z$) and P-F (Li_xPF_y), indicating a stable artificial SEI film can be constructed by introducing a LPO layer. In the F 1s XPS curves (Figs. 4e and f), the C-F peak at 688.16-688.26 eV is derived from PVDF [43], which is consistent with C 1s curves. In addition, Li-F bond at 685.37-685.22 eV is detected in both electrodes due to the decomposition of $LiPF_6$ [44], but more Li-F can be detected in ALD-LPO-0 cathode. As can be seen from the chemical Eqs. 1-3, there are two main sources of Li-F. The first source is mainly LiF generated by direct decomposition of electrolyte. The other part originates from the by-product PF_5 of electrolyte decomposition, which further reacts with water to produce POF_3, and then reacts with Li_2O to produce LiF or Li_xPOF_y. It can be known that the reduction of Li-F content infers the decreased decomposition of electrolyte. As a result, the SEI at the interface between electrolyte and cathode no longer becomes thicker. As such, the accumulation of undesirable products at the interface between electrolyte and cathode is reduced, helping to provide a better intercalation and deintercalation path for lithium ion.

To sum up, dense ionic conductor LPO coating layers were uniformly deposited on NCM9064 cathodes by applying ALD technique. Long cycling performance the LPO covered NCM9064 electrode at room and high temperature were significantly improved. Moreover, rate performance of modified NCM9064 cathode materials were also greatly promoted when the thickness of LPO coating layer was optimized. The roles of the LPO coating could be concluded as: (1) A physical barrier layer to build a mechanically robust network, helping to reduce the stress expansion of whole cathode and direct contact between the cathode material and the electrolyte; (2) A chemical inert and electrochemically stable layer with strong P-O chemical bond and fast lithium ion conducting property, benefiting to constructing a stable SEI film free of HF corrosion. To sum up, the ALD introduction of a uniform and thin polyanionic ionic conductor layer (such as LPO) will be a promising covering strategy for improve the performance of Ni-rich material-based electrodes.

Declaration of competing interests

The authors declare that they have no known competing financial interests or personal relationships that could have appeared to influence the work reported in this paper.

Acknowledgments

This work was supported by the National Natural Science Foundation of China (No. 52174285), the Science and Technology Innovation Program of Hunan Province (No. 2022RC3048), the Key Research and Development Program of Yunnan Province (No. 202103AA080019), and the Research Foundation of Education Bureau of Hunan Province (No. 18B477).

Supplementary materials

Supplementary material associated with this article can be found, in the online version, at doi:10.1016/j.cclet.2023.108638.

References

[1] W. Li, E.M. Erickson, A. Manthiram, Nat. Energy 5 (2020) 26–34.
[2] Y. Xia, J. Zheng, C. Wang, et al., Nano Energy 49 (2018) 434–452.
[3] M. Malik, K.H. Chan, G. Azimi, Mater. Today Energy 28 (2022) 101066.
[4] X. Wang, B. Zhang, Z. Xiao, et al., Chin. Chem. Lett. 34 (2023) 107772.
[5] J. Liu, J. Wang, Y. Ni, et al., Mater. Today 43 (2021) 132–165.
[6] X. Tan, W. Peng, G. Luo, et al., Mater. Today Energy 29 (2022) 101114.
[7] Y. Lv, S. Huang, Y. Zhao, et al., Appl. Energy 305 (2022) 117849.
[8] J.W. Kim, K. Jung, T. Yim, J. Mater. Sci. Technol. 86 (2021) 70–76.
[9] F. Wu, D. Zhou, L. Zhang, et al., J. Mater. Chem. A 10 (2022) 11437–11448.
[10] S. Liu, J. Su, C. Zhang, et al., Mater. Today Energy 10 (2018) 40–47.
[11] M. Zybert, H. Ronduda, K. Dąbrowska, et al., Energy Reports 8 (2022) 3995–4005.
[12] Z. Wang, H. Zhu, H. Yu, et al., Chin. Chem. Lett. 34 (2023) 107718.
[13] S. Jamil, L. Yue, C. Li, et al., Chem. Eng. J 441 (2022) 135821.
[14] D.A. Lim, Y.K. Shin, J.H. Seok, et al., ACS Appl. Mater. Interfaces 14 (2022) 54688–54697.

[15] G.J. Chung, Y.H.T. Tran, J. Han, et al., Chem. Eng. J 446 (2022) 137288.
[16] M. Yee, K. An, D.T. Nguyen, et al., Mater. Today Energy 24 (2022) 100950.
[17] S.J. Sim, S.H. Lee, B.S. Jin, et al., J. Power Sources 481 (2021) 229037.
[18] Q. Yang, J. Huang, Y. Li, et al., J. Power Sources 388 (2018) 65–70.
[19] Y.S. Jung, A.S. Cavanagh, L.A. Riley, et al., Adv. Mater. 22 (2010) 2172–2176.
[20] Z. Guo, X. Zhang, M. Wang, et al., Chem. Eng. J 431 (2022) 134031.
[21] X. Li, J. Liu, M.N. Banis, et al., Energy Environ. Sci. 7 (2014) 768–778.
[22] L. Zhao, G. Chen, Y. Weng, et al., Chem. Eng. J. 401 (2020) 126138.
[23] Z. Ahaliabadeh, V. Miikkulainen, M. Mantymaki, et al., ACS Appl. Mater. Interfaces 13 (2021) 42773–42790.
[24] L. Wang, Q. Su, W. Shi, et al., Electrochim. Acta 435 (2022) 141411.
[25] X. Wang, J. Cai, Y. Ren, et al., Energy Chem. 69 (2022) 531–540.
[26] G. Dai, H. Du, S. Wang, et al., RSC Adv. 6 (2016) 100841–100848.
[27] Y. Shi, Y. Xing, K. Kim, et al., Electrochem. Soc. 168 (2021) 040501.
[28] J.H. Kim, J.S. Park, S.H. Cho, et al., J. Mater. Chem. A 10 (2022) 25009–25018.
[29] H. Yang, M. Ku, J. Kim, et al., ACS Appl. Energy Mater. 5 (2022) 8313–8323.
[30] P. Darapaneni, A.U. Mane, Z.D. Hood, et al., ACS Appl. Energy Mater. 5 (2022) 9870–9876.
[31] J. Ahn, E.K. Jang, S. Yoon, et al., Appl. Surf. Sci. 484 (2019) 701–709.
[32] Y. Liu, X. Wang, J. Cai, et al., J. Mater. Sci. Technol. 54 (2020) 77–86.
[33] J. Liang, S. Hwang, S. Li, et al., Nano Energy 78 (2020) 105107.
[34] S. Deng, X. Li, Z. Ren, et al., Energy Storage Mater. 27 (2020) 117–123.
[35] F. Tian, L. Ben, H. Yu, H. Ji, et al., Nano Energy 98 (2022) 107222.
[36] G. Cherkashinin, M. Motzko, N. Schulz, et al., Chem. Mater. 27 (2015) 2875–2887.
[37] Y.C. Lu, A.N. Mansour, N. Yabuuchi, et al., Chem. Mater. 21 (2009) 4408–4424.
[38] A.M. Andersson, A. Henningson, H. Siegbahn, et al., J. Power Sources 119-121 (2003) 522–527.
[39] R. Genieser, S. Ferrari, M. Loveridge, et al., J. Power Sources 373 (2018) 172–183.
[40] T.F. Yi, L.Y. Qiu, J. Mei, et al., Sci. Bull. 65 (2020) 546–556.
[41] H. Bouayad, Z. Wang, N. Dupré, et al., J. Phys. Chem. C 118 (2014) 4634–4648.
[42] K. Edström, T. Gustafsson, J.O. Thomas, Electrochim. Acta 50 (2004) 397–403.
[43] X. Yu, Y. Wang, H. Cai, et al., Ionics 25 (2019) 1447–1457.
[44] J. Im, J. Lee, M.H. Ryou, et al., J. Electrochem. Soc. 164 (2017) A6381–A6385.